INL/CON-13-29589
PREPRINT

Differentiating the Role of Lithium and Oxygen in Retaining Deuterium on Lithiated Graphite Plasma-Facing Components

Physics of Plasmas, 2013

C. N. Taylor
J. P. Allain
K. E. Luitjohan
P. S. Krstic
J. Dadras
C. H. Skinner

November 2013

The INL is a
U.S. Department of Energy
National Laboratory
operated by
Battelle Energy Alliance

Differentiating the role of lithium and oxygen in retaining deuterium on lithiated graphite plasma-facing components

C.N. Taylor[1,2], J.P. Allain[2,3], K.E. Luitjohan[2], P.S. Krstic[4,5,6], J. Dadras[5,7], C.H. Skinner[8]

[1]*Fusion Safety Program, Idaho National Laboratory, P.O. Box 1625-7113 Idaho Falls, ID 83415, USA*
[2]*School of Nuclear Engineering, Purdue University, 400 Central Drive, West Lafayette, Indiana 47907, USA*
[3]*Department of Nuclear, Plasma and Radiological Engineering, University of Illinois at Urbana-Champaign, IL 61801*
[4]*Institute for Advanced Computational Science, Stony Brook University, NY 11794*
[5]*Department of Physics and Astronomy, University of Tennessee, Knoxville, TN 37996*
[6]*TheoretiK, Knoxville, TN 379XX*
[7]*Department of Chemistry & Biochemistry, University of California Los Angeles, Los Angeles CA 90095*
[8]*Princeton Plasma Physics Laboratory, Princeton, NJ 08543*

Abstract

Laboratory experiments have been used to investigate the fundamental interactions responsible for deuterium retention in lithiated graphite. Oxygen was found to be present and play a key role in experiments that simulated NSTX lithium conditioning, where the atomic surface concentration can increase to >40% when deuterium retention chemistry is observed. Quantum-classical molecular dynamic simulations elucidated this oxygen-deuterium effect and showed that oxygen retains significantly more deuterium than lithium in a simulated matrix with 20% lithium, 20% oxygen, and 60% carbon. Simulations further show that deuterium retention is even higher when lithium is removed from the matrix. Experiments artificially increased the oxygen content in graphite to ~16% and then bombarded with deuterium. XPS showed depletion of the oxygen and no enhanced deuterium retention, thus demonstrating that lithium is essential in retaining the oxygen that thereby retains deuterium.

I. INTRODUCTION

Plasma-surface interactions in magnetically confined fusion devices are intimately linked to global plasma performance. In large part, most phenomena associated with this connection relate to the transfer of impurities from the plasma to the first wall or from the walls to the plasma. Much effort is routinely expended in fusion devices to condition the walls and plasma in order to reduce undesired impurities.[1]

Many methods for wall conditioning have been implemented.[2] A first-order technique for wall conditioning is to pre-treat plasma-facing components (PFC) prior to plasma operations. Vacuum surfaces are typically physically cleaned and then baked in vacuum to release adsorbed contaminants. A second-order technique involves discharge-cleaning techniques that use energetic particles (frequently He). These glow discharges help desorb hydrogen from the walls and may be used on a daily or per-shot basis.

A third-order method of wall conditioning involves adding material to the walls in order to getter and tightly bind impurities. Thin Ti films were initially used in a number of fusion devices[3] but were prone to cracking and peeling, thus introducing more serious impurities into the plasma. Chromium and beryllium films have also been used.[3-5] Plasma-assisted chemical vapor deposition has been used to condition PFCs with carbon, silicon, and boron for the same purposes.[6,7] Through this evolutionary process the now apparent trend became obvious; materials that remove or strongly bind oxygen to the surface yielded a plasma with fewer impurities and better performance.[1] In addition, low-Z elements pose less risk for radiative losses. Ironically, however, lithium was initially suspected to not be an effective oxygen getter in the presence of hydrogen due to its binding energy being less than that of water.[1]

The use of lithium for wall conditioning began empirically as lithium pellets were initially introduced into TFTR during transport experiments.[8-10] The added lithium yielded unanticipated improvements in energy confinement time, fusion power, stored energy, and the Lawson triple product $nT\tau_E$.[11,12] Since then, lithium has been used in CDX-U[13], FTU[14], DIII-D[15], TJ-II[16], T-11M[17], EAST[18], and NSTX.[19] NSTX has pioneered and advanced lithium wall conditioning over a phased effort.

The first phase of lithium wall conditioning in NSTX began in 2004 when the lithium pellet injector (LPI) was installed.[20] The LPI was capable of injecting several mg of

lithium into plasma discharges. Results indicated that improvements lasted only one or two shots and then performance reverted to pre-lithium conditions. In view that 'more is better', the next phase of the lithium campaign introduced lithium via a lithium evaporator (LiTER) in 2006, and a second LiTER was added the following year for a total lithium evaporation rate of 10-40 mg/min.[21] During the 2007 campaign a total of ~93 g lithium had been deposited in NSTX. Then in 2010 a liquid lithium divertor (LLD) was added to NSTX that was filled using the LiTERS, and then resistively heated. Little difference in impurity pumping was observed during use of the LLD, although this is likely a result of the evaporative lithium coating parts of the vessel other than the LLD.[22] Analysis of these results is ongoing.

Similar to earlier methods of wall conditioning (e.g., titaniumization, siliconization, boronization, etc.), from the onset of its use, lithium conditioned walls have been found to reduce carbon and oxygen impurities in the plasma, and prevent deuterium from recycling back into the plasma. Preliminary laboratory experiments revealed much about lithiated graphite phenomena, such as intercalation and oxygen gettering, however the underlying mechanisms responsible for these improvements were unknown.[23,24] Experiments in the PISCES-B linear plasma device made great efforts to achieve a clean liquid lithium surface in order to understand the mechanisms of deuterium retention.[25] These results suggested that deuterium binds in lithium in the form of LiD. However, lithium coating of graphite does not easily allow for a *clean* lithium surface due to intercalation and oxygen gettering. Experiments both in off-line facilities and with an in-situ PMI probe on NSTX demonstrated the importance of surface impurities in the emission of molecular species during TDS measurements of the same. Skinner et al. showed a dominant emission channel of HDO and Nieto-Perez et al. correlated behavior with oxygen and deuterium.[26,27] Consequently the fundamental mechanisms for deuterium retention in lithiated graphite remained unknown until recently.

The purpose of this paper is to summarize the recent series of results that have led to the identification of the fundamental interactions responsible for deuterium retention in lithiated graphite and to differentiate the role of oxygen and lithium in retaining deuterium. As the use of lithium has become prolific, these results apply not only to plasma physics, but also to the fields of lithium batteries, hydrogen storage and nano-

electronics, among others.[28,29]

II. THE SURFACE CHEMISTRY OF IRRADIATED LITHIATED-GRAPHITE

In order to reveal and understand the fundamental mechanisms responsible for deuterium retention in lithiated graphite, this matrix has been examined using primarily X-ray photoelectron spectroscopy (XPS) and quantum-classical molecular dynamic (QCMD) simulations. The methods of these techniques have been explained in detail elsewhere.[30-34] The chemistry of the graphite surface is experimentally analyzed and changes are measured as lithium is deposited and deuterium is introduced. It is noteworthy to mention that XPS has a probing depth of 1-10 nm, depending on the substrate being examined, and is not able to detect deuterium directly due to the low probability of electron emission from hydrogen. Instead, deuterium is detected indirectly through its interactions with other constituents. For example, a new peak forms in the oxygen (O 1s) energy region when lithiated graphite is bombarded by deuterium. The formation of this new peak is indicative of new surface chemistry and can be directly attributed to the chemical interaction of deuterium with the matrix constituents. This method allows XPS to be used to directly explore the deuterium binding chemistry with oxygen.

The recent effort to understand the fundamental nature of deuterium retention in lithiated graphite has taken a multi-facet approach as illustrated in Figure 1. 1) Graphite tiles were analyzed in order to investigate what happened to the lithium-deuteirum surface chemistry during an NSTX campaign.[31] 2) A materials analysis particle probe (MAPP) has been designed to assess the real-time effect of individual plasma shots.[35,36] MAPP will introduce samples in-vacuo to the plasma facing surface for plasma exposure and immediately retracted for analysis. 3) Atomistic simulations are used to test and predict the retention capacity of future PFC matrices.[32] 4) Offline laboratory experiments connect each of these facets and the combination of these has yielded a synergistic step in understanding the fundamental mechanisms responsible for retaining deuterium in lithiated graphite.

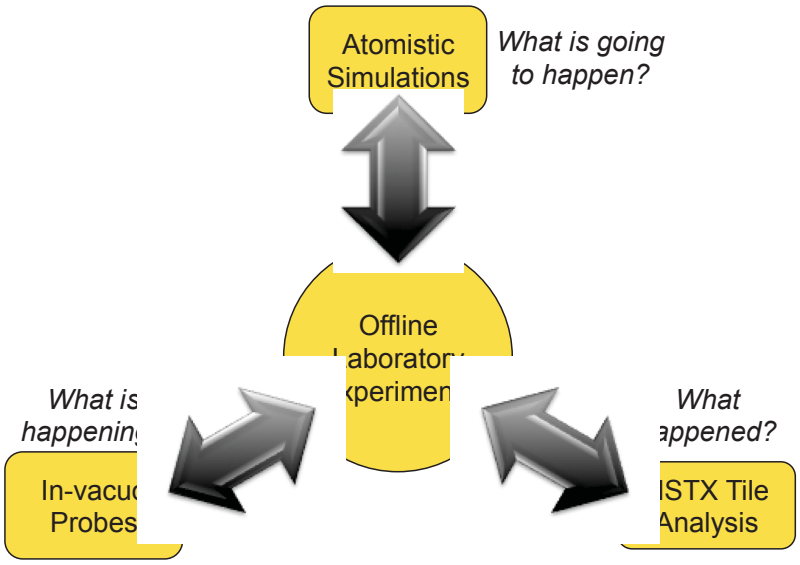

Figure 1. Researching the fundamental mechanisms of deuterium retention in lithiated graphite uses multiple approaches, each connected through offline laboratory experiments.

A. Offline laboratory experiments

Several important trends were immediately identified in initial experiments with lithiated graphite.[30] Though not a new discovery, the oxygen natively found in ATJ graphite (at 532 eV, produced from an oxygen electron in a C-O bond) typically accounted for ~5% of the atomic surface concentration. Depositing lithium promptly increased this fraction by a factor of two (on average) and also resulted in the formation of a second XPS peak in the O1s region (Li–O, at ~529.5 eV). Offline experiments typically used a nominal deposited lithium thickness of 2 μm to compare with end-of-campaign NSTX tiles that had accumulated many μm of lithium. By comparing the relative intensity of the two O1s peaks, the native C–O peak with the post-lithium deposition Li–O peak, XPS could be used to monitor intercalation and oxygen gettering [see Figure 3 in Ref. (30)]. In the first hour after depositing lithium, intercalation was observed as the Li-O intensity decreased relative to the C–O intensity in a 1 μm nominal lithium deposit on graphite. Similarly, by comparing this ratio during the first hour after a 5 μm lithium dose was deposited, the Li–O intensity increased relative to the C–O intensity, thus indicating oxygen gettering. Gettering was also found to occur on a longer time scale as a lithitated graphite sample sat in UHV. Over the course of ~300 hr, the oxygen content increased to account for more than 20% of the total surface

concentration.[34]

Even after depositing 5 μm lithium, carbon was still observed using XPS. It seemed strange that with such a thick "layer" of lithium on graphite, that the surface concentration showed anything but lithium and oxygen. However, atomic force and scanning electron micrographs of the polished mirror-like laboratory samples showed mountainous micron surface features (see Fig. 3 in Ref. 34). The rough surface increased the surface area and effectively thinned the lithium deposit. This combined with rapid intercalation allowed the carbon to appear in XPS.

The challenge of lithium intercalation into graphite was also tested by Maingi et al. who found that small amounts of lithium deposition had a linear correlation to an improvement in plasma performance.[37] This result raised the importance of time scales in the measurement of surface chemistry of lithiated graphite. In Figure 2,**Error! Reference source not found.** in-situ low-energy ion scattering spectroscopy (LEISS) was performed during lithium evaporation. Each scan used 2 keV He^+ at sample-normal incidence and took about 2 minutes. In this data it is clear that depositing lithiated coatings can maintain a significant amount of lithium at the top surface so long as fresh lithium is continually deposited. Once deposition ends, oxygen atoms accumulate on the lithium surface. In NSTX the possibility of continuous erosion of Li-C films from the surface and its re-deposition along the field lines in the lower divertor could also be envisaged as a source of "fresh" lithium layers deposited by the coupled state of the plasma and its interface with the lithiated graphite tiles in NSTX. Understanding the role of segregating lithium and oxygen atoms during and after lithium deposition, and subsequent irradiation is the subject of current studies.

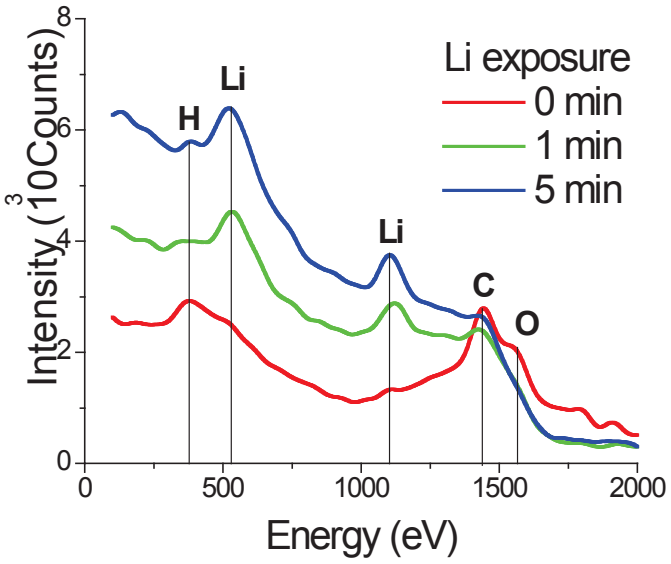

Figure 2. Low energy ion scattering spectroscopy (LEISS) showing the chemistry of the top monolayer during lithium deposition on graphite. The times listed represent the time into lithium deposition.

After identifying these oxygen related trends, lithiated graphite was exposed to more fusion relevant conditions: deuterium ion bombardment. The control to this experiment[30] was to bombard virgin graphite (no lithium) with deuterium. By controlling lithium, its effect on deuterium bombardment and consequently deuterium retention could be assessed, thus allowing identification of the XPS peaks where deuterium retention was made manifest. Specifically, deuterium interacts prominently within the oxygen O1s region (Li–O–D, at ~533 eV) in the XPS spectrum. Deuterium interactions were also found within the carbon C1s region (Li–C–D, at ~291.2 eV), but to a lesser extent. The changes in the lithium Li1s region in response to deuterium irradiation were found to be much more subtle. Little interpretation was originally provided regarding the Li1s spectra, however subsequent analysis helped clarify its behavior as will be presented in Figure 3.

Incrementing the deuterium fluence between XPS scans was used to investigate the saturation behavior of lithiated graphite by deuterium.[38] It was found that the formation of the Li–O–D peak came at the expense of the consumption of the Li–O peak. As the deuterium fluence increased, the Li–O–D/Li–O peak ratio increased until the sample stopped responding to further deuterium bombardment, at which point (~5×10^{17} cm^{-2}) the lithiated graphite sample was said to have become saturated with deuterium. A similar

analysis was performed by examining the C1s peak ratios, which was found to saturate at a slightly lower fluence ($2.5x10^{17}$ cm^{-2}). To evaluate the effect of 5 sec NSTX-U pulses on lithium saturation, this study should be extended to fluences in excess of 10^{18} cm^{-2}.

Initially the indiscriminate shifting of the Li1s peak upon deuterium bombardment revealed little information. However, through analyzing NSTX tiles and peak deconvolution, details regarding the Li1s spectra were recognized and are presented herein. Figure 3 shows the Li1s photoelectron spectrum of laboratory produced lithiated-graphite after various stages of deuterium irradiation. In both the 30 min and 1.5 hr deuterium irradiation steps, prominent shoulders are observed, which point to two convoluted peaks. Peak deconvolution reveals a peak at 54.8 eV, corresponding to lithium metal, and another peak at 56.3 eV. At 1.5 hr the peak at higher energy begins to dominate the spectrum. Hoenigman and Keil found that a peak near 56 eV formed when lithium was exposed to water vapor and an indistinguishable peak also formed when exposing lithium to molecular oxygen.[39] Since the 56.3 eV peak in Figure 3 grows upon deuterium irradiation (compare with Fig 1 in Ref. 38), and given its association with water vapor,[39,40] we identify this peak as an Li-O-D interaction, whereas the lower energy peak is attributed to lithium metal.[41]

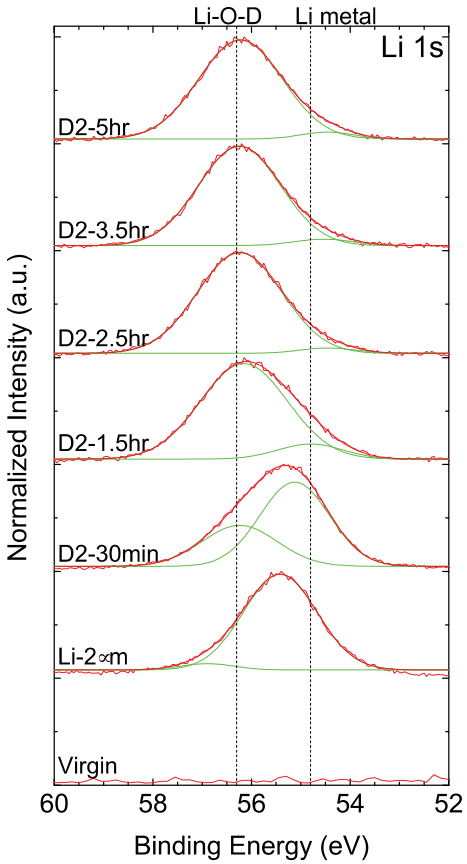

Figure 3. XPS LI 1s spectra of virgin graphite (ATJ147), after 2 µm lithium deposition, and after D_2 irradiation fluences: 30 min (9.0 x 10^{16} cm^{-2}), 1.5 h (2.5 x 10^{17} cm^{-2}), 2.5 h (3.8 x 10^{17} cm^{-2}), 3.5 h (5.2 x 10^{17} cm^{-2}), and 5.0 h (7.2 x 10^{17} cm^{-2}). The Li-O-D peak (56.3 ± 0.6 eV) enhances as the Li metal peak diminishes (at 54.8 ± 0.6 eV) as the deuterium fluence increases.

B. NSTX tile analysis

NSTX tiles were removed following the 2008 campaign and compared with results obtained in offline laboratory experiments.[31] Tiles had been exposed to thousands of plasma shots with countless variations in parameters and wall conditions. Upon removal, the tiles were exposed to air and passivated. XPS was used to examine the tile samples in their as-received state, and after various cleaning steps that were used to remove the passivated layers. The cleaning steps actually used depended on the sample origin from within NSTX. Most samples reached a clean state after Ar sputtering, while some samples, specifically those found nearest the intersection of the lower divertor and center stack, required annealing in addition to Ar sputtering. Figure 4 shows the peak evolution during Ar sputter cleaning of a NSTX tile sample. The as-received spectra were similar

to those reported by Harilal, et al.[42] The deuterium related chemistry was revealed in the O1s, C1s, and Li1s regions as demonstrated in their characteristic Li–O–D (533 eV), Li–C–D (291.2 eV), and Li–O–D (~56.3 eV) peaks, respectively.

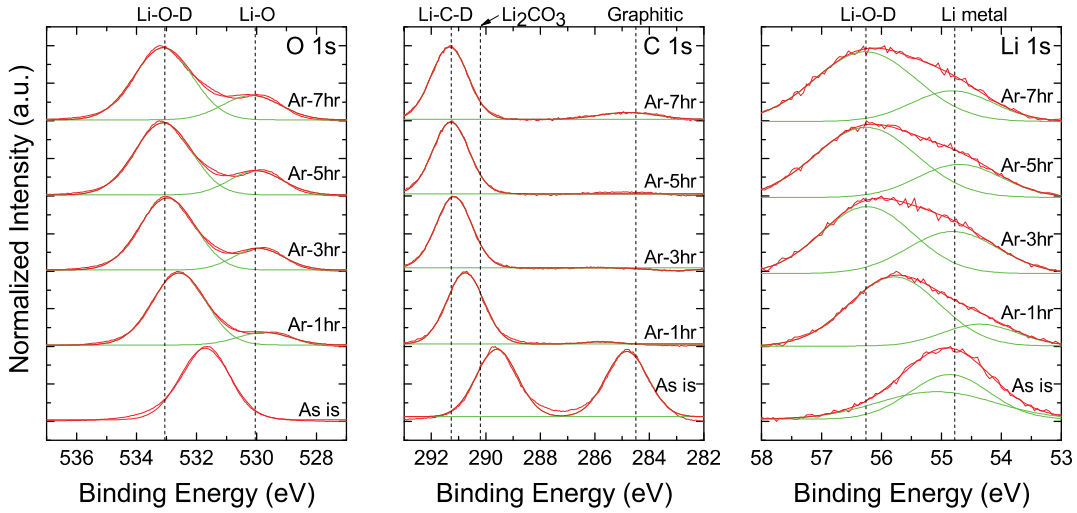

Figure 4. XPS spectra of NSTX tiles after various Ar sputter cleaning steps.

Dual peaks were observed in the O1s and Li1s energy regions. As sputter cleaning progressed, the relative intensity of the dual O1s and Li1s peaks changed. The ratio between the Li–O–D peaks relative to the total O1s and Li1s peak areas is plotted in Figure 5. The downward trend in the O1s region indicates that the deuterium resides primarily in surface layers since it can be easily removed via sputtered. Li–O–D is also observable in the Li1s range, and one would assume that deuterium removal would likewise be observed during Ar sputtering. However the Li–O–D/Li1s peak ratio shows an opposite upward trend. Hoenigman and Keil showed that lithium oxide and lithium hydroxide have indistinguishable XPS spectra.[39] The upward Li–O–D/Li1s trend is suspected to be an artifact of this convolution.

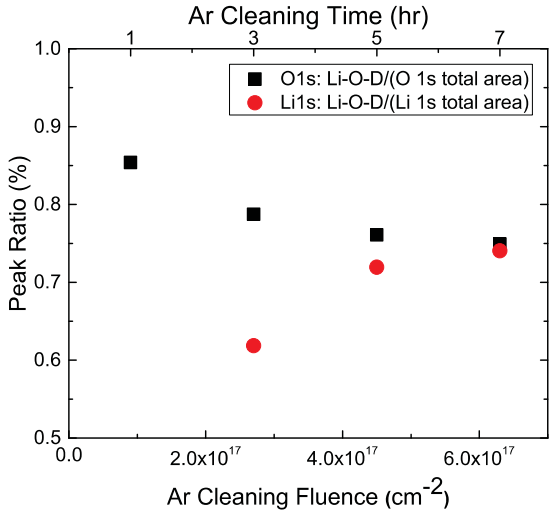

Figure 5. Li-O-D peaks appear in the O1s and Li1s XPS regions. The upward trend in the Li1s peak ratio is suspected to be an artifact of indistinguishable lithium oxide and lithium hydroxide peaks as discussed in Ref. [39].

The as-received spectra for samples found within approximately ±4 cm of the lower divertor-center stack intersection exhibited XPS spectra uncharacteristic of lithiated graphite.[31] Ar sputtering was not able to reveal the deuterium chemistry in NSTX tile sample with such spectra. Previous work [31] showed that a series of Ar sputtering and annealing to ~550 C was capable of revealing the deuterium related chemistry. Figure 6 shows the reverse cleaning process where the sample was heated to 360ºC, 450ºC, and 550ºC prior to Ar sputtering. Heating in these steps incrementally shifted the spectra towards the peak positions corresponding with deuterium retention. Subsequent Ar

sputtering further revealed the Li–O peak in the O1s region. Samples from this region had some unique plasma processing that was not observed elsewhere in other tiles that were analyzed, and this behavior could not be replicated in offline laboratory experiments.

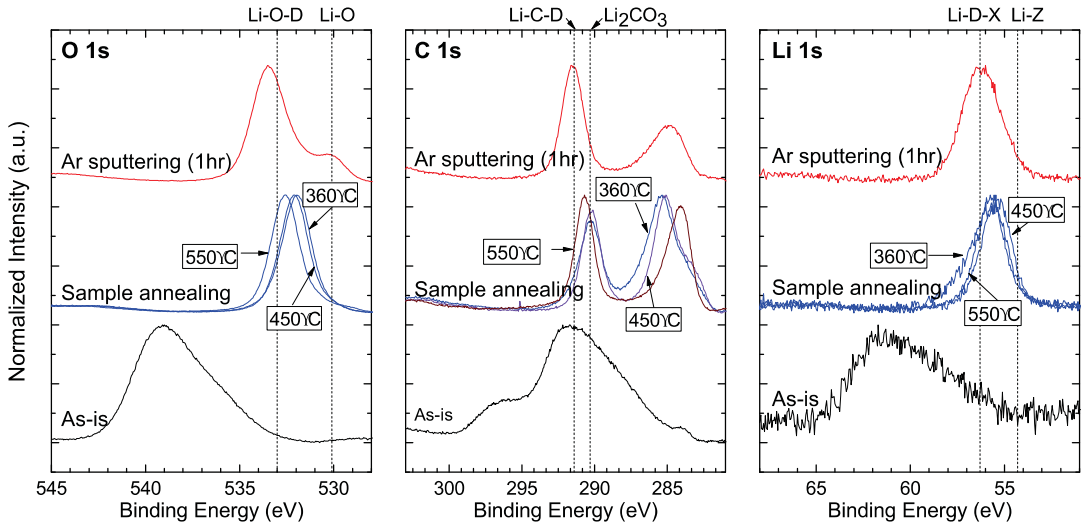

Figure 6. Incrementally heating NSTX tile samples removed from nearest the lower inner divertor begins to reveal the Li–O–D chemistry observed in offline laboratory experiments.

NSTX tile analysis also revealed important information that connected the tile surface chemistry to plasma performance.[31] Specifically, based on the relative intensity of the Li–O–D XPS peaks, regions of high and low sputtering were identified, pointing to areas that should require additional lithium conditioning in order to contribute to enhanced deuterium pumping. XPS also showed that all known deuterium-related surface chemistry can be desorbed through heating to ~830ºC. Information was ascertained regarding minimum lithium thresholds. A particular tile sample with low lithium coverage did not reveal deuterium related chemistry while an adjacent sample did exhibit deuterium interactions. Complementary experiments identified that a minimum lithium threshold dose of ~100-500 nm was necessary to retain deuterium in lithiated graphite.[31]

C. In-vacuo probes

Offline laboratory experiments and post-campaign tile analysis are not capable of replicating or distinguishing the effect of individual plasma discharges. In order to do so, in-vacuo probes have been designed for NSTX and NSTX-U.[26,35,36] The first sample analysis probe (SAP) consisted of a linear actuator that inserted four samples to the lower

divertor surface. The system contained only one diagnostic, a residual gas analyzer (RGA) for thermal desorption spectroscopy (TDS), and was intended to test the feasibility of implementing a more advanced system. Initial TDS results were presented in Refs. [26,36] and showed two desorption peaks, which pointed to a weak and, more prominently, a strong retention mechanism.

The materials analysis particle probe (MAPP) built on the success of the SAP and utilized the same four-specimen sample holder (Figure 7) and TDS system (RGA and sample heater). MAPP added additional diagnostics and a custom designed chamber.[36] A compact hemispherical energy analyzer, X-ray source, and low energy ion source (≤1000 eV) were added to provide additional surface analysis techniques. The X-ray source has enabled near surface (<10 nm) chemical characterization, and it is planned to interrogate the top monolayer through ion scattering spectroscopy (ISS) and detect hydrogen concentrations via direct recoil spectroscopy (DRS).[36] MAPP is currently being used and tested on the lithium tokamak experiment (LTX) in preparation for the completion and startup of NSTX-U later this year.

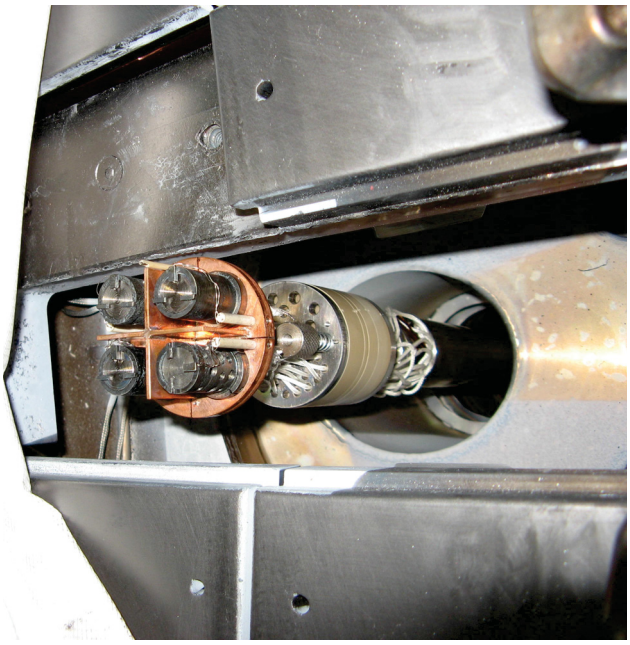

Figure 7. Photograph of the MAPP sample holder inserted to the plasma facing surface in NSTX.

D. Atomistic simulations

Laboratory experiments identified the dynamic nature of lithitated graphite and the significant changes in the atomic surface concentrations that were observed after deuterium bombardment. It was conjectured that the chemistry of the intercalated lithium in carbon was playing a key role in the increased deuterium retention and the decreased carbon erosion observed in fusion devices. However, the mechanism was not clear until calculations[32] showed that oxygen chemistry was primarily responsible for bonding deuterium and carbon more strongly to the mixed carbon/lithium matrix, while lithium was playing a catalyzing role, to bring and retain the oxygen in the matrix. It also followed from calculations that the surface content of oxygen had to be well above the oxygen concentration in virgin graphite (~5%) in order to yield significant effects.[33] The experiments[32] that followed found that concentrations of oxygen in a thin layer of the lithiated carbon surface upon bombardment by deuterium indeed reached 20-40%. This oxygen then enables enhanced chemistry, caused by reactivity of oxygen with D and C, and particularly with Li. The oxygen attaches itself with strong, mixed covalent-ionic bonds to both C, D and Li, keeping together atoms in the surface mixture. This results in the suppression of C erosion and increasing retention of impacting and penetrating D atoms.

Composition	%	%	%	%	%
C	100	80	60	52	80
Li		20	20	16	
O			20	16	20
H				16	
Eject (C) yield	0.36	0.93	0.20	0.17	0.10
Retain	77.17	75.77	84.57	87.18	87.71

Table I. Calculated ejection and retention rates (per impact D) for various prepared mixtures of C, Li, O and H.

These conclusions were obtained after performing many quantum-classical molecular dynamics calculations with the software package DFTB on various, predefined, amorphous compositions (shown at Table I) of the C, O, Li and D atoms bombarded by low-energy D atoms.[32,33] Table I presents the ejection yields of carbon, and retention

probabilities of D upon bombardment of the matrices by D. The presence of lithium in the carbon matrix actually deleteriously decreases deuterium retention and even increases ejection of carbon, in comparison to the bare carbon matrix. However, the presence of oxygen in the matrix (last three columns in Table I) significantly both suppresses ejection of carbon and increases the retention of impacting D.

The details of the calculations were presented in our previous publications.[32-34] Evolving the system of atoms in the small time steps (0.2 fs), at each step the nuclei are "frozen", the electron structure of the system is solved quantum-mechanically, then effective potentials and forces are determined for atoms, and lastly the atoms are allowed to move under these forces for the next 0.2 fs. The system is evolved for a few hundred ps, until the retained D atoms reach their bonding equilibrium. This is repeated for five thousand independent D impacts in order to obtain statistically valid results. Although we used the self-consistent charge, density functional tight-binding approximation, the numerical intensity of the quantum-mechanical calculations limited the matrix size to a few hundred atoms. This was sufficient to obtain qualitative conclusions however the absolute numbers may differ to the experimentally obtained ones. Analyzing "charge neutralization" and the "nearest neighbors" of the deuterium projectiles allowed the assessment of likely deuterium binding pairs.[32,33]

These results corroborated offline laboratory experiments, leading to the conclusion that oxygen, as long as it is present in relatively high quantities, is primarily responsible for enhanced deuterium retention. However, plasma performance improves in fusion devices that use lithium wall conditioning, which supports the notion that more lithium is better.[37] Given that oxygen has been found to be primarily responsible for enhanced deuterium retention, the precise role that lithium holds becomes a curiosity. This will be discussed in the next section.

III. DIFFERENTIATING THE ROLE OF LITHIUM AND OXYGEN

Since computational results showed that oxygen-deuterium binding is the dominant mechanism for deuterium retention, with or without lithium in the matrix, it is reasonable to hypothesize that the same results would be observed in experiments if the oxygen concentration could be artificially increased to the 16-20% range used in simulations,

even in absence of lithium. In order to increase the O1s surface concentration, an ATJ graphite sample was irradiated with a 2000 eV oxygen ion beam (referred to as oxygenated-graphite) and immediately characterized by XPS. Figure 8 shows that after a $5x10^{17}$ cm^{-2} oxygen bombardment, the graphite's oxygen surface concentration increased from 4.9% to 16.4%. This value was comparable with the 16-20% oxygen concentrations used in the simulations, Table I, where enhanced oxygen-deuterium binding was observed. Immediately after conducting the ~20 min XPS scan, the sample was then irradiated with a low flux ($4.8x10^{12}$ $cm^{-2}s^{-1}$) 1000 eV deuterium ion beam. The ion energy was chosen such that the projected deuterium ion range would overlap with the range of the implanted oxygen.[43] Since our atomistic model showed the dominant mechanism for deuterium retention to be related to oxygen, we expected to see a dramatic enhancement of the deuterium related O1s peak (533 eV) during this deuterium irradiation just as we had observed with lithiated graphite.[30] However, after the oxygenated-graphite was irradiated with deuterium to a fluence of $6x10^{15}$ cm^{-2}, 63% of the implanted oxygen was removed and continuing deuterium irradiation to $1x10^{17}$ cm^{-2} removed all implanted oxygen. At this point, as shown in Figure 8, no deuterium retention peaks were observed in the C1s region. In the O1s region, peak deconvolution placed a peak close to where deuterium retention was observed in lithiated graphite (533 eV). However the very low intensity of the O1s peak (4.7 at.%) ensures that little if any deuterium could be retained.

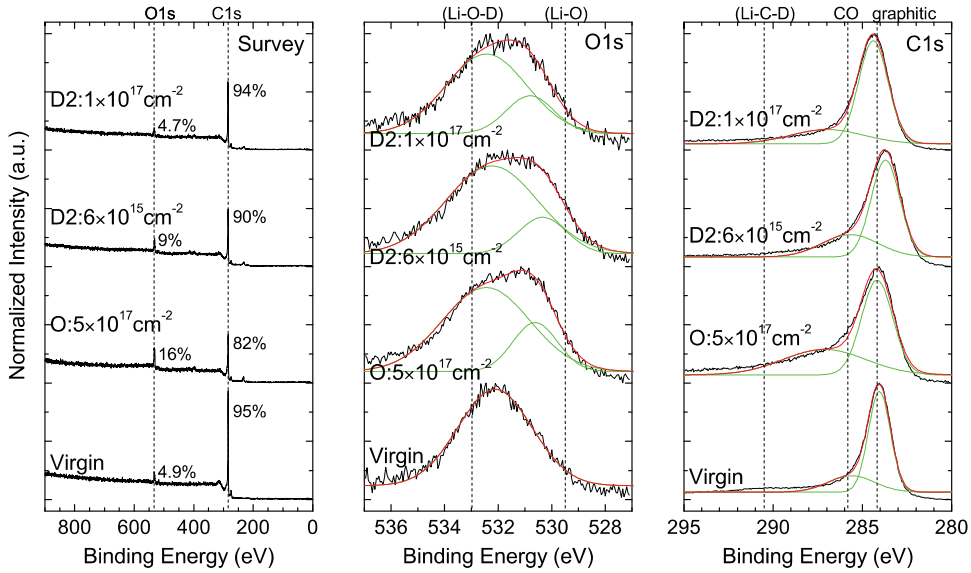

Figure 8. Bombarding ATJ graphite with an oxygen ion beam (125 eV/amu) increases the oxygen surface concentration to ~16%, however subsequent deuterium bombardment (500 eV/amu) removes the implanted oxygen. Ion energies were chosen to have overlapping penetration depths.

Although oxygen bombardment did successfully increase the O1s surface concentration, the rapid loss of surface oxygen during deuterium irradiation indicated that the graphite was unable to maintain large amounts of oxygen without a retaining medium (i.e., lithium). At first, this result appeared to be inconsistent with the model, as simulations showed that lithium was not necessary for enhanced deuterium retention. However, the case for oxygen etching from graphite by deuterium bombardment was an effect measured in a time-scale of seconds to minutes during experiments. Comparison to our computational atomistic simulations, which comprise prompt effects of the order of less than nanoseconds, is too short of a time scale for oxygen release to take place. Secondly, while qualitatively yielding the same chemistry (see Fig. 3 in Ref. [32]), simulations were performed with deuterium impact energy of 5 eV, which was too low for any significant etching of oxygen from graphite.

Figure 9 compares the O1s surface concentration of three ATJ graphite samples each with different surface treatments: namely, deuterium irradiation of virgin graphite (triangle), deuterium irradiation of Li-graphite (circle), and deuterium irradiation of oxygenated-graphite (square). The virgin graphite sample shows a *decrease* in oxygen surface concentration after deuterium irradiation. The Li-graphite sample (circles) sees a slight oxygen increase following lithium deposition and a *dramatic increase* in surface

oxygen after D-irradiation. In contrast, although oxygen irradiation (squares) successfully increases the oxygen concentration to levels used in the simulations, deuterium irradiation triggers prompt release of the implanted oxygen. This confirms the indispensable role of lithium in binding the oxygen in the carbon matrix, even upon D bombardment. Similarly it helps explain why conditioning with lithium results in improved confinement of tokamak plasmas even though oxygen is the primary component to chemically bind with the incident energetic deuterium.

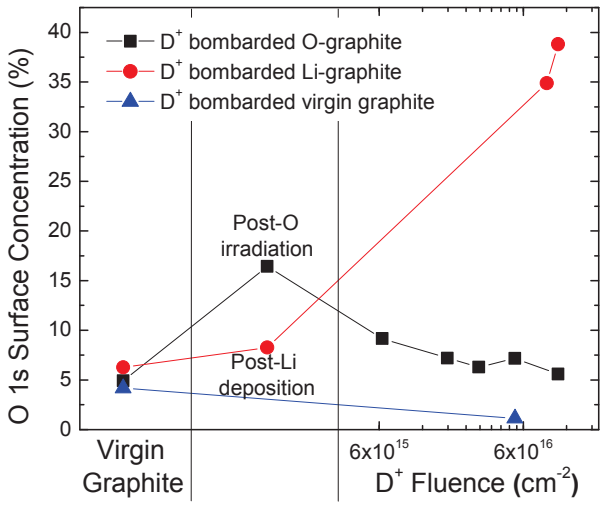

Figure 9. Deuterium bombardment of virgin graphite (blue triangle) removes surface oxygen. In lithiated graphite, deuterium irradiation dramatically increases the oxygen concentration (red circle). Oxygen irradiation (black square) increases the oxygen surface concentration to ~16%; however, subsequent low-fluence deuterium irradiation ($6x10^{15}$ cm^{-2}) releases 63% of implanted oxygen. Lines shown to guide the eye.

IV. CONCLUSIONS

The surface chemistry of lithiated graphite changed dynamically across various parameters. Most notably, the oxygen concentration increased over the course of 100s of hours as lithium getters oxygen. Deuterium retention was observed in the photoelectron energy spectrum for lithiated graphite in three locations. In the O1s region, retention was observed at 533 eV in the form of Li–O–D interactions, in the C1s region at ~291.2 eV in the form of Li–C–D interactions, and in the Li1s region at ~56 eV as Li–O–D interactions.

Atomistic simulations demonstrated that oxygen is the dominant channel for retaining deuterium, and that lithium surprisingly does not significantly contribute to enhanced deuterium retention.[32,33] Instead, these enhancements were observed when large

quantities of oxygen are present. To validate these atomistic models, we artificially and successfully increased graphite's oxygen concentration to 16% through oxygen ion bombardment. Then, to test the retention capability of this oxygenated-graphite sample, the sample was bombarded with deuterium ions. Instead of deuterium retention, rapid oxygen removal was observed at the surface with our *in-situ* characterization. Without lithium, the graphite could not sustain a large concentration of oxygen at the surface. Therefore, oxygen is required to retain deuterium, but lithium is required to retain oxygen at the surface. We conclude that lithium changes the effective release mechanisms of oxygen under deuterium irradiation. Without lithium conditioning, deuterium irradiation induces surface etching of oxides from graphite. With lithium conditioning, more oxygen is available at the surface which leads to higher deuterium uptake at the surface.

These results also extend beyond the context of lithiated graphite in fusion devices; they establish that several ingredients are required in order to achieve high deuterium (hydrogen) uptake. In experiments by Lee et al., various alkalis were evaporated on Ge, however results suggested that lithium is a more efficient oxygen getter even though higher-Z alkalis have a lower electronegativity.[44] The second consideration is the substrate. If solely relying on thermodynamic processes (i.e., not ion irradiation), the immediate interaction depth is limited to the top few monolayers. Therefore, the substrate morphology, and consequently the surface area, is an important consideration[45] since a larger surface adsorbs more oxygen. These effects are enhanced in carbon since alkalis intercalate into carbon allotropes[46] and further increase the oxygen interaction volume.

Acknowledgements

CNT acknowledges financial supported by U.S. DOE Contract No. DE-FG02-08ER54990 and DE-AC07–05ID14517. JPA acknowledges financial support by U.S. DOE Contract No. DE-FG02-08ER54990. PSK and JD acknowledges support of the Laboratory Directed Research and Development (LDRD) program of the Oak Ridge National Laboratory. The computed data were obtained at the DOE computational resources of the NCCS (Jaguar) and at NSF computational resources of the NICS (Kraken). PSK and JD acknowledge computer support of the DOE INCITE program and

NSF Xsede program. CS acknowledges support from US DOE Contract No. DE AC02-09CH11466.

References

[1] J. Winter, Plasma Phys. Control. Fusion **38**, 1503 (1996).
[2] H.F. Dylla, J. Nucl. Mater. **93**, 61 (1980).
[3] J. Winter, J. Nucl. Mater. **161**, 265 (1989).
[4] P. Mioduszewski, J.E. Simpkins, P.H. Edmonds, R.C. Isler, E.A. Lazarus, C.H. Ma, M. Murakami, and A.J. Wootton, J. Nucl. Mater. **128-129**, 884 (1984).
[5] H.F. Dylla, P.H. LaMarche, W.R. Blanchard, R.V. Budny, F.P. Boody, C.E. Bush, R.J. Groebner, P.J. McCarthy, J.E. Simpkins, and B.C. Stratton, Journal of Vacuum Science & Technology a: Vacuum, Surfaces, and Films **4**, 1753 (1986).
[6] L. Peng, E. Wang, N. Zhang, D. Yan, M. Wang, Z. Wang, B. Deng, K. Li, J. Luo, and L. Liu, Nuclear Fusion **38**, 1137 (1998).
[7] J. Winter, J. Nucl. Mater. **145**, 131 (1987).
[8] J.L. Terry, E.S. Marmar, J.A. Snipes, D. Garnier, and V.Y. Sergeev, Rev. Sci. Instrum. **63**, 5191 (1992).
[9] J.L. Terry, E.S. Marmar, R.B. Howell, M. Bell, A. Cavallo, E. Fredrickson, A. Ramsey, G.L. Schmidt, B. Stratton, and G. Taylor, Rev. Sci. Instrum. **61**, 2908 (1990).
[10] V.Y. Sergeev, E.S. Marmar, J.A. Snipes, J.L. Terry, H. Park, D.K. Mansfield, M. Bell, and D. McCune, Rev. Sci. Instrum. **63**, 4984 (1992).
[11] D.K. Mansfield, K.W. Hill, J.D. Strachan, M.G. Bell, S.D. Scott, R. Budny, E.S. Marmar, J.A. Snipes, J.L. Terry, and S. Batha, Physics of Plasmas **3**, 1892 (1996).
[12] D.K. Mansfield, J.D. Strachan, M.G. Bell, S.D. Scott, R. Budny, E.S. Marmar, J.A. Snipes, J.L. Terry, S. Batha, R.E. Bell, M. bitter, C.E. Bush, Z. Chang, D.S. Darrow, D. Ernst, E. Fredrickson, B. Grek, H.W. Herrmann, K.W. Hill, A. Janos, D.L. Jassby, F.C. Jobes, D.W. Johnson, L.C. Johnson, F.W. Levinton, D.R. Mikkelsen, D. mueller, D.K. Owens, H. Park, A.T. Ramsey, A.L. Roquemore, C.H. Skinner, T. Stevenson, B.C. Stratton, E. Synakowski, G. Taylor, A. von Halle, S. von Goeler, K.L. Wong, and S.J. Zweben, Physics of Plasmas **2**, 4252 (1995).
[13] R. Majeski, M. Boaz, D. Hoffman, B. Jones, R. Kaita, H. Kugel, T. Munsat, J. Spaleta, V.A. Soukhanovskii, J. Timberlake, L. Zakharov, G. Antar, R.P. Doerner, S. Luckhardt, R.W. Conn, M. Finkenthal, D. Stutman, R. Maingi, and M. Ulrickson, Fusion Engineering and Design **65**, 443 (2003).
[14] A.A. Tuccillo, A. Alekseyev, B. Angelini, S.V. Annibaldi, M.L. Apicella, G. Apruzzese, J. Berrino, E. Barbato, A. Bertocchi, A. Biancalani, W. Bin, A. Botrugno, G. Bracco, S. Briguglio, A. Bruschi, P. Buratti, G. Calabrò, A. Cardinali, C. Castaldo, C. Centioli, R. Cesario, L. Chen, S. Cirant, V. Cocilovo, F. Crisanti, R. De Angelis, U. de Angelis, L. Di Matteo, C. Di Troia, B. Esposito, G. Fogaccia, D. Frigione, L. Gabellieri, F. Gandini, E. Giovannozzi, G. Granucci, F. Gravanti, G. Grossetti, G. Grosso, F. Iannone, H. Kroegler, V. Lazarev, E. Lazzaro, I.E. Lyublinski, G. Maddaluno, M. Marinucci, D. Marocco, J.R. Martin-Solis, G. Mazzitelli, C. Mazzotta, V. Mellera, F. Mirizzi, S. Mirnov, G. Monari, A. Moro, V. Muzzini, S. Nowak, F.P. Orsitto, L. Panaccione, D. Pacella, M. Panella, F. Pegoraro, V. Pericoli-Ridolfini, S. Podda, S. Ratynskaia, G. Ravera, A. Romano, A. Rufoloni, A. Simonetto, P. Smeulders, C. Sozzi, E. Sternini, B. Tilia, O. Tudisco, A. Vertkov, V. Vitale, G. Vlad, R. Zagórski, M. Zerbini, and F. Zonca, Nuclear Fusion **49**, 104013 (2009).
[15] G.L. Jackson, E.A. Lazarus, G.A. Navratil, R. Bastasz, N.H. Brooks, D.T. Garnier, K.L. Holtrop, J.C. Phillips, E.S. Marmar, and T.S. Taylor, J. Nucl. Mater. **241**, 655 (1997).

[16] J. Sánchez, F.L. Tabarés, D. Tafalla, J.A. Ferreira, I. García-Cortés, C. Hidalgo, F. Medina, M.A. Ochando, and M.A. Pedrosa, J. Nucl. Mater. **390**, 852 (2009).
[17] S.V. Mirnov, V.B. Lazarev, S.M. Sotnikov, V.A. Evtikhin, I.E. Lyublinski, and A.V. Vertkov, Fusion Engineering and Design **65**, 455 (2003).
[18] G.S. Xu, B.N. Wan, J.G. Li, X.Z. Gong, J.S. Hu, J.F. Shan, H. Li, D.K. Mansfield, D.A. Humphreys, V. Naulin, international collaborators, Nuclear Fusion **51**, 072001 (2011).
[19] M.G. Bell, H.W. Kugel, R. Kaita, L.E. Zakharov, H. Schneider, B.P. LeBlanc, D. mansfield, R.E. Bell, R. Maingi, S. Ding, S.M. Kaye, S.F. Paul, S.P. Gerhardt, J.M. Canik, J.C. Hosea, G. Taylor, the NSTX research team, Plasma Phys. Control. Fusion **51**, 124054 (2009).
[20] G. Gettelfinger, J. Dong, R. Gernhardt, H. Kugel, P. Sichta, and J. Timberlake, Fusion Engineering, 2003. 20th IEEE/NPSS Symposium on 359 (2003).
[21] H.W. Kugel, M.G. Bell, J.W. Ahn, J.P. Allain, R. Bell, J. boedo, C. Bush, D. Gates, T. Gray, S. kaye, R. Kaita, B. leblanc, R. Maingi, R. Majeski, D. mansfield, J. menard, D. mueller, M. Ono, S. paul, R. Raman, A.L. Roquemore, P.W. Ross, S. Sabbagh, H. Schneider, C.H. Skinner, V.A. Soukhanovskii, T. Stevenson, J. Timberlake, W.R. Wampler, and L. Zakharov, Physics of Plasmas **15**, 056118 (2008).
[22] H.W. Kugel, M.G. Bell, J.P. Allain, R.E. Bell, S. Ding, S.P. Gerhardt, M.A. Jaworski, R. Kaita, J. Kallman, S.M. Kaye, B.P. LeBlanc, R. Maingi, R. Majeski, R. Maqueda, D.K. Mansfield, D. mueller, R. nygren, S.F. Paul, R. Raman, A.L. Roquemore, S.A. Sabbagh, H. Schneider, C.H. Skinner, V.A. Soukhanovskii, C.N. Taylor, J.R. Timberlake, W.R. Wampler, L.E. Zakharov, S.J. Zweben, and T.N.R. Team, J. Nucl. Mater. 1 (2010).
[23] H. Sugai, H. Toyoda, K. Nakamura, K. Furuta, M. Ohori, K. Toi, S. Hirokura, and K. Sato, J. Nucl. Mater. **220-222**, 254 (1995).
[24] H. Sugai, M. Ohori, and H. Toyoda, Vacuum **47**, 981 (1996).
[25] M.J. Baldwin, R.P. Doerner, S.C. Luckhardt, and R.W. Conn, Nuclear Fusion **42**, 1318 (2002).
[26] C.H. Skinner, J.P. Allain, W. Blanchard, H.W. Kugel, R. Maingi, A.L. Roquemore, V.A. Soukhanovskii, and C.N. Taylor, J. Nucl. Mater. **415**, S773 (2011).
[27] M. Nieto-Perez, J.P. Allain, B. Heim, and C.N. Taylor, J. Nucl. Mater. **415**, S133 (2011).
[28] J.R. Dahn, T. Zheng, Y. Liu, and J.S. Xue, Science **270**, 590 (1995).
[29] K. Srinivasu and S.K. Ghosh, The Journal of Physical Chemistry C **116**, 5951 (2012).
[30] C.N. Taylor, B. Heim, and J.P. Allain, Journal of Applied Physics **109**, 053306 (2011).
[31] C.N. Taylor, K.E. luitjohan, B. Heim, L. Kollar, J.P. Allain, C.H. Skinner, H.W. Kugel, R. Kaita, A.L. Roquemore, and R. Maingi, Fusion Engineering and Design (2013).
[32] P.S. Krstic, J.P. Allain, C.N. Taylor, J. dadras, S. Maeda, K. Morokuma, J. Jakowski, A. Allouche, and C.H. Skinner, Phys. Rev. Lett. **110**, 105001 (2013).
[33] P.S. Krstic, J.P. Allain, A. Allouche, J. Jakowski, J. dadras, C.N. Taylor, Z. Yang, K. Morokuma, and S. Maeda, Fusion Engineering and Design **87**, 1732 (2012).
[34] C.N. Taylor, J. Dadras, K.E. luitjohan, J.P. Allain, P.S. Krstic, and C.H. Skinner, Journal of Applied Physics **114**, 223301 (2013).
[35] B. Heim, S. Gonderman, C.N. Taylor, J.P. Allain, Z.C. Yang, M. Gonzalez, E. Collins, C.H. Skinner, B. Ellis, W. Blanchard, A.L. Roquemore, H.W. Kugel, R. Martin, and R. Kaita, IEEE Trans. Plasma Sci. **40**, 735 (2012).
[36] C.N. Taylor, B. Heim, S. Gonderman, J.P. Allain, Z. Yang, R. Kaita, A.L. Roquemore,

C.H. Skinner, and R.A. Ellis, Rev. Sci. Instrum. **83**, 10D703 (2012).
[37] R. Maingi, S.M. Kaye, C.H. Skinner, D.P. Boyle, J.M. Canik, M.G. Bell, R.E. Bell, T.K. Gray, M.A. Jaworski, R. Kaita, H.W. Kugel, B.P. LeBlanc, D.K. Mansfield, T.H. Osborne, S.A. Sabbagh, and V.A. Soukhanovskii, Phys. Rev. Lett. **107**, 145004 (2011).
[38] C.N. Taylor, J.P. Allain, B. Heim, P.S. Krstic, C.H. Skinner, and H.W. Kugel, J. Nucl. Mater. **415**, S777 (2011).
[39] J.R. Hoenigman and R.G. Keil, Applications of Surface Science **18**, 207 (1984).
[40] C.H. Skinner, R. Sullenberger, B.E. Koel, M.A. Jaworski, and H.W. Kugel, J. Nucl. Mater. **438**, S647 (2013).
[41] D. Ensling, A. Thissen, and W. Jaegermann, Scripta Materialia **255**, 2517 (2008).
[42] S.S. Harilal, J.P. Allain, A. Hassanein, M.R. Hendricks, and M. Nieto-Perez, Applied Surface Science **255**, 8539 (2009).
[43] J.F. Ziegler, J.P. Biersack, M.D. Ziegler, The Stopping and Range of Ions in Matter, SRIM Co., 2008. www.SRIM.org.
[44] G. Lee, J.Y. Lee, S. Kim, and E.J. Cho, Surface Science **532-535**, 764 (2003).
[45] D. den Engelsen and B. Ferrario, J. Vac. Sci. Technol. B **22**, 809 (2004).
[46] M. Caragiu and S. Finberg, J. Phys.: Condens. Matter **17**, R995 (2005).